Polymer/Laponite Composite Colloids through Emulsion Polymerization: Influence of the Clay Modification Level on Particle Morphology

Norma Negrete-Herrera,[†] Jean-Luc Putaux,[‡] Laurent David,[§] and Elodie Bourgeat-Lami*,[†]

Laboratoire de Chimie et Procédés de Polymérisation, UMR 140 CNRS/ESCPE, Bât. 308F, 43 Bd. du 11 Novembre 1918, BP 2077, 69616 Villeurbanne Cedex, France; Centre de Recherches sur les Macromolécules Végétales, UPR 5301 CNRS, BP 53, F-38041 Grenoble Cedex 9, France; and Laboratoire des Matériaux Polymères et Biomatériaux, UMR CNRS 5627 IMP, Bât. ISTIL, Université Claude Bernard Lyon 1, 69622 Villeurbanne Cedex, France

Received May 10, 2006; Revised Manuscript Received September 28, 2006

ABSTRACT: A series of composite latexes have been synthesized by seeded emulsion (co)polymerization of styrene and butyl acrylate in the presence of Laponite clay particles previously functionalized by ion exchange with a free radical initiator: 2,2-azobis(2-methylpropionamidine) hydrochloride (AIBA). Since the AIBA/Laponite intercalation complexes settled down in water immediately after cation exchange, a set of experiments was first carried out in order to establish the conditions required to obtain stable aqueous dispersions of organically modified Laponite. Dynamic light scattering (DLS) and small-angle X-ray scattering (SAXS) were used to monitor the evolution of particle size and analyze the properties of the aqueous suspensions as a function of the amount of intercalated cation. A series of composite latexes were then prepared by emulsion polymerization using the organoclays as seeds. The composite particles were characterized by cryo-transmission electron microscopy (cryo-TEM), and a particular effort was devoted to analyze the effect of the Laponite modification level on particle morphology.

Introduction

During the past 10 years, there has been an increased interest in the synthesis of polymer nanocomposites characterized by inorganic particles dispersed into polymeric matrices.[1−5] Since the optical, thermal, rheological, and mechanical properties of these materials strongly depend on the techniques used for their elaboration, a variety of synthetic strategies have been reported worldwide with the aim to control dispersions of the inorganic filler within the host polymer. Among the wide range of nanostructured materials, efforts have focused in recent years on the elaboration of polymer-layered silicate (PLS) nanocomposites using natural and synthetic clay minerals.[6−9] Again, considerable effort has been made to develop synthetic methods that allow precise control over the composite's nanostructure. Three main routes are currently reported: exfoliation/adsorption, in-situ intercalative polymerization, and melt intercalation. All three strategies usually require pretreatment of the clay mineral in order to improve its compatibility with the polymer matrix and achieve a good dispersion. This can be realized for instance by treating the clay with silane coupling agents as demonstrated in recent works from our group.[10,11] Organic compounds can also be incorporated into the interlayer galleries through an ion exchange process. Ion exchange reactions with cationic surfactants including primary, tertiary, and quaternary ammonium ions render the silicate surface hydrophobic, which makes possible the subsequent intercalation of a variety of monomers and/or polymers. Alternatively, the alkylammonium cations can provide functional reactive groups (e.g., monomers, initiators, catalysts, etc.) that can participate in the polymerization and promote exfoliation of the clay layers.

There has been a great number of reports on the synthesis of nanocomposites by in-situ intercalative polymerization.[12−18] However, these approaches mainly produce polymeric solutions of exfoliated clay sheets and do not give rise to particles. Thus, attempts to synthesize PLS latexes through emulsion polymerization have been recently described in the open literature.[19−31] This heterophase polymerization process offers many advantages compared to solution or bulk polymerizations such as a low viscosity of the suspension medium, high polymer molecular weights, and the possibility to control particles morphology. In addition, the latex route seems particularly well suited in order to produce homogeneous dispersions of clay minerals into polymer matrices by taking advantage of the swelling behavior of clay platelets in water. Finally, it is worth reminding that emulsion polymers can find applications in a variety of domains including waterborne adhesives, paints, and coating formulations. However, to the best of our knowledge, there exist only few reports dealing with the incorporation of ion-exchanged clays into emulsion polymers. In one of these reports, Meneghetti and Qutubuddin[31] described the synthesis of PMMA−clay nanocomposites via emulsion polymerization at 60 °C using Montmorillonite (MMT) functionalized by either a zwitterionic surfactant (octadecyldimethylbetaine), a cationic surfactant (benzalkonium chloride), or an anionic surfactant (sodium dodecyl sulfate) through ion exchange. They showed that the nanoparticles morphology and the latex properties were both affected by the nature of the interaction between the surfactant and the clay surface. In a related work, Choi et al.[19] reported the synthesis of PMMA/Na-MMT nanocomposites through emulsion polymerization of methyl methacrylate (MMA) using 2-acrylamido-2-methyl-1-propanesulfonic acid (AMPS) or so-

[†] UMR 140 CNRS/ESCPE.
[‡] UPR 5301 CNRS.
[§] UMR CNRS 5627 IMP.
* Corresponding author: e-mail bourgeat@lcpp.cpe.fr, Tel 33 (0)4 72 43 17 77; Fax 33 (0)4 72 43 17 68.

10.1021/ma0610515 CCC: $33.50
Published on Web 11/23/2006

Table 1. AIBA Adsorption onto Laponite[a]

samples	C_{AIBA} added (mmol L^{-1}_{water})	C_{AIBA} added (mmol $g^{-1}_{Laponite}$)	C_{AIBA} (% of CEC)	C_{AIBA} free (mmol L^{-1}_{water})	C_{AIBA} adsorbed (mmol $g^{-1}_{Laponite}$)
AIBA-Lap-57	2.14	0.214	57	0.05	0.209
AIBA-Lap-118	4.42	0.442	118	0.88	0.354
AIBA-Lap-200	7.52	0.752	200	3.79	0.373

[a] [Laponite] = 10 g L^{-1}_{water}.

dium dodecylbenzenesulfonate as surfactants. Both surfactants were intercalated into the Na-MMT layers. The organoclay was then dispersed into water before polymerization. When AMPS was used as surfactant, the clay platelets were exfoliated during polymerization as evidenced by TEM analysis. However, no mention was made of the morphology of the resulting nanoparticles.

In this paper, we hereby report the synthesis of poly(styrene-*co*-butyl acrylate)/Laponite nanocomposite latexes through emulsion polymerization. Laponite was functionalized by ion exchange with a cationic initiator (AIBA) which role is to promote polymer chains growth at its surface. In our previous works, we have shown that the resulting particles mainly consisted of latex spheres recovered by exfoliated clay sheets.[11,32] To gain insight into the parameters of the process that allows controlling the particles (nano)structure, we aim in this report to investigate in more depth the influence of the level of modification of Laponite on the morphology of the poly(sty-*co*-BuA)/Laponite composite particles and on the colloidal stability of the resulting suspensions. To that purpose, Laponite clay platelets were modified by AIBA at three different concentrations, e.g., below the cation exchange capacity (CEC) of the clay, around the CEC, and above the CEC. The organoclays were dispersed into water, and the resulting suspensions were used as seeds to produce the composite latexes.

Experimental Procedures

Materials. The synthetic clay selected in this study was Laponite RD (Rockwood Additives Ltd.). The monomers, styrene and butyl acrylate (from Aldrich), were distilled in a vacuum before use to remove the inhibitor. The 2,2-azobis(2-methylpropionamidine) hydrochloride cationic initiator (AIBA, M_w = 271.2 g mol^{-1}, Acros Organics), the surfactant sodium dodecyl sulfate (SDS, Acros Organics), and the peptizing agent tetrasodium pyrophosphate ($Na_4P_2O_7$, Sigma Aldrich) were used as supplied. The water was purified using a Milli-Q Academic system (Millipore Corp.) (conductivity 18.2 μS and pH 6.8).

Methods. *(a) Organic Modification of Laponite.* The organoclays were prepared from Laponite RD by cation exchange using 2,2-azobis(2-methylpropionamidine) hydrochloride (AIBA) as organic cation at three different concentrations corresponding to 57%, 118%, and 200% the CEC of Laponite, respectively. The resulting intercalation complexes will be hereinafter referred to as AIBA-Lap-57, AIBA-Lap-118, and AIBA-Lap-200. In a typical experiment, the cation exchange was carried out as follows: 2 g of Na^+−Laponite was added to 200 mL of deionized water and stirred for ~3 h until the obtention of a free-flowing and transparent suspension. Then, the required amount of AIBA, calculated on the basis of the CEC value of Laponite and the M_w of AIBA (Table 1), was added to the clay suspension under magnetic stirring. The mixture was stirred at room temperature for 24 h. The resulting white precipitate was isolated by filtration, and the supernatant solution was analyzed by chemical titration to determine the residual AIBA concentration. The adsorbed amount was deduced by difference between the initial and the residual AIBA concentrations as reported previously.[32]

(b) Aqueous Dispersions of Ion-Exchanged Laponite. Redispersion was performed by adding directly known amounts of SDS and $Na_4P_2O_7$ to the clay precipitate. The dispersions were stirred magnetically for 48 h, and their size was determined by dynamic light scattering (DLS). A series of experiments were performed in order to evaluate the effect of the concentration of the peptizing agent and of the agitation time on the organoclay particles size for different AIBA concentrations.

(c) Seeded Emulsion Polymerization Using the Ion-Exchanged Laponite Particles as Seeds. Emulsion polymerization was carried out in a 250 mL three-necked double-wall reactor equipped with a condenser, a nitrogen inlet tube, and a stirrer. In a typical experiment, butyl acrylate (7 g) and styrene (3 g) were introduced into 100 g of the aqueous suspension of ion-exchanged Laponite (1 g) containing the surfactant (SDS, 2 g L^{-1}) and the peptizing agent ($Na_4P_2O_7$, 1 g L^{-1}). The emulsion was sonicated for 2 min using a Bransson W450 digital sonifier (95% output power). The final mixture was introduced in the reactor and deoxygenated by heating to 70 °C while purging with nitrogen. This was considered to be the beginning of polymerization.

Characterizations. A JEOL JCXA 733 electron microprobe analyzer (EPMA) was used to determine the carbon content of the supernatant solutions after cation exchange. Small-angle X-ray scattering (SAXS) studies were performed at the bending magnet-based anomalous diffusion and diffraction beamline BM02-D2AM, at the European Synchrotron Radiation Facility (ESRF) in Grenoble, France. For liquid samples, the analysis was performed on dilute (10 g L^{-1}) aqueous suspensions using low-density polyethylene insulin syringes of 0.5 mL. A 3 mm diameter hole was drilled close to the basis and perpendicular to the long axis of each syringe and then sealed by an adhesive polyimide Kapton film. The data were collected as reported previously.[10] For cryomicroscopy observations, the hybrid nanoparticles were observed embedded in a thin film of vitreous ice, using Philips CM200 cryo-transmission electron microscope (cryo-TEM) according to a procedure described elsewhere.[33−35] The diameters of the organically modified Laponite clay particles and of the polymer latexes were measured by dynamic light scattering (DLS) using a Malvern Autosizer Lo-C instrument with a detection angle of 90°. Monomer conversions were determined gravimetrically. Typically, 3−7 g of the latex suspension was placed in an aluminum dish and dried to constant weight at 110 °C.

Results and Discussion

Intercalation of AIBA into Sodium Laponite. The clay used in the present work is Laponite RD. Laponite is a trioctahedral 2:1 layered silicate structurally related to the naturally occurring hectorite but free from the extraneous elements which are normally present in samples of that mineral. Since Laponite is a cationic exchanger, organic cations adsorb on the negative charges that are present in the clay structure. Source of negative charges in Laponite are both from isomorphic substitution (permanent charges) and broken edges (pH dependent). Isomorphic substitution is due to substitution within the lattice structure of lithium ions by magnesium ions. The edges of Laponite particle are pH dependent due to the presence of amphoteric groups (MgOH, LiOH, and SiOH). These surface groups may be protonated or deprotonated depending on the pH value of the surrounding solution. While MgOH and LiOH are positively charged below pH = 9, SiOH groups are negatively charged.[36−39] The amount of negative charges, defined as the cation exchange capacity of the clay (CEC), is one of the fundamental properties of clay materials. In the case

of Laponite, it is equal to 0.75 mequiv g^{-1}.[39] It should be noticed that the edge charges represent less than 10% of the CEC of the mineral.[39]

The cation-exchange was carried out using 2,2-azobis(2-methylpropionamidine) hydrochloride (AIBA) as cationic initiator. Note that as this molecule carries two positive amidinium charges, 1 equiv of AIBA can potentially exchange two sodium cations. When the aqueous solution of AIBA was added to the aqueous clay suspension, an immediate flocculation of the clay particles was observed which enabled the easy determination of the residual cation concentration in the upper supernatant solution. An additional centrifugation of the clay suspension was performed in order to ensure a complete phase separation. The amount of AIBA electrostatically bonded to the clay surface was determined by chemical titration of the supernatant solution (Table 1). At loadings below the CEC of the clay (AIBA-Lap-57), almost the totality of AIBA was adsorbed onto Laponite (there was no free AIBA in solution). When the loading was increased to values close to the CEC (AIBA-Lap-118) or greater than the CEC (AIBA-Lap-200), the adsorbed amounts increased to values corresponding to full exchange of the sodium cations. Note that the use of an excess of AIBA (AIBA-Lap-200) had only a minor effect on the extent of adsorption.

Aqueous Dispersions of Organically Modified Laponite. It is known that at moderate concentration and low ionic strength, Laponite completely exfoliates in aqueous solutions.[40] In contrast, the ion-exchanged Laponite samples are strongly aggregated and no longer swell in the presence of water. This behavior suggests that the hydration of the intercalated cation is too small to overcome the van der Waals attraction energy between the unit layers. However, in a previous article, we have demonstrated that a stable aqueous clay suspension was necessary to produce stable latexes.[11] Therefore, a set of experiments was carried out in order to establish the conditions required to obtain stable aqueous dispersions of organically modified Laponite for different levels of organic modification. All dispersions were prepared at a fixed clay concentration of 10 g L^{-1} under magnetic stirring. In the case of the AIBA-Lap-57 sample, no precipitate was found, and instead, we observed the formation of a viscous gel. In contrast, precipitation occurred in the case of the AIBA-Lap-118 and the AIBA-Lap-200 samples. Note that in every case no particle size could be determined by DLS. From these results, it was clear that additional effort was needed in order to achieve an acceptable level of dispersion of the organoclay in water.

The quality of the dispersions could be significantly improved by introducing a peptizing agent in the suspension. Commercially, peptizers are added to raw Laponite powders in order to retard clay aggregation when the latter is suspended in water (giving rise to the so-called "sol grade"). These molecules are generally multivalent ion salts that bind specifically to the edges of the Laponite platelets. In the case of tetrasodium pyrophosphate ($Na_4P_2O_7$), which was the peptizer used in our study, this tetravalent negatively charged ion adsorbs onto the positively charged rims and thereby effectively screens the rim charge. A set of aqueous dispersions of AIBA-Lap-118 with a clay concentration of 10 g L^{-1} and different concentrations of $Na_4P_2O_7$ was prepared and characterized by DLS (Figure 1). As expected, the results indicate that the aggregation is strongly reduced or inhibited by the addition of the peptizing agent. It must be pointed out that the higher the $Na_4P_2O_7$ concentration between 0 and 1.5 g L^{-1}, the smaller the particles size. However, no effect was observed at higher concentrations.

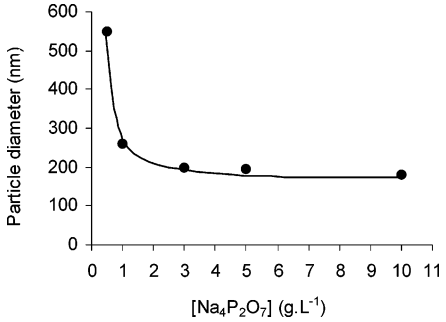

Figure 1. Effect of the $Na_4P_2O_7$ concentration on the average particle diameter of 10 g L^{-1} aqueous dispersions of AIBA-Lap-118.

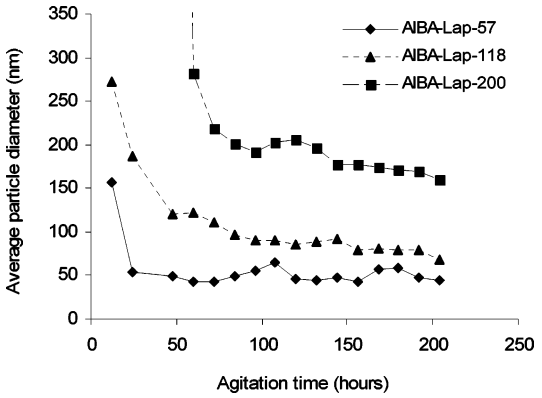

Figure 2. Evolution of the average particle diameter as a function of the agitation time of a series of AIBA−Laponite suspensions with increasing levels of modification.

To go one step further, a kinetic study on the evolution of the particle size of ion-exchanged Laponite as a function of the agitation time was performed in order to reach the smallest size as possible. A series of AIBA-Laponite complexes were dispersed in water at the concentration of 10 g L^{-1}. According to the previous results, the aqueous suspensions were prepared by adding 1 g L^{-1} of $Na_4P_2O_7$, which corresponds to the minimum peptizer concentration for which we observed a significant decrease in particle size (in order to avoid a too high ionic strength). In addition, in this series of experiments, the suspensions were sonicated for 120 s at 90% output power to promote clay exfoliation. Figure 2 shows the evolution of the average particle diameter vs the agitation time for increasing AIBA loadings. In the case of the AIBA-Lap-57 sample, the particle size decreased down to about 50 nm after only 1 day of agitation. This result is quite satisfactory if we consider that the particle size of raw Laponite is ∼30 nm. In contrast, the AIBA-Lap-118 sample needs more time to achieve a constant particle size (3 days), and the final value was higher than for the AIBA-Lap-57 sample (ca. 90 nm). Since in this case the AIBA concentration was slightly higher than the CEC of Laponite, the anionic surface charges of the clay were completely neutralized which rendered clay redispersion much more difficult. The particle size of the intercalated Laponite clay samples containing the highest AIBA concentration (AIBA-Lap-200) could not be determined by DLS after 3 days of agitation even after ultrasonication of the clay suspension. Particle size decreased progressively with time and reached a minimum value of ∼200 nm after 125 h (e.g., around 5 days).

In summary, we considered that the optimal particle size of 10 g L^{-1} aqueous dispersions of AIBA-intercalated Laponites was reached in the presence of 1 g L^{-1} of $Na_4P_2O_7$ at room temperature and after 1, 3, and 5 days of magnetic agitation for

AIBA-Lap-57, AIBA-Lap-118, and AIBA-Lap-200, respectively.

Synchrotron SAXS. Further insights into the structure of the organically modified Laponite suspensions elaborated under optimal conditions and increasing AIBA concentrations were provided by synchrotron SAXS. The derived plots of log(I) vs log(q) for ion-exchanged and raw Laponites (not shown here) exhibit a slope close to -2 at high q values, but in a limited scattering range (between $q = 4 \times 10^{-2}$ up to about 0.3 Å^{-1}), which is consistent with the dispersion of lamellar particles with random orientation. Therefore, the SAXS data were analyzed using expressions derived by Guinier and Fournet.[41] In the case of AIBA-functionalized Laponite suspensions, the values of the slope of the scattering curves are comparable but become steeper with increasing AIBA loadings. A similar behavior has been observed for high Laponite concentrations.[42] The theory considers that the scattering intensity per unit volume, $I(q)$, produced from a two-phase system under dilute conditions (which means that the structure factor arising from interference effects may be neglected) is given by

$$I(q) = \Delta\rho^2\phi P(q) = (\rho_1 - \rho_2)^2\phi P(q) \quad (1)$$

where q is the scattering vector defined as $q = 4\pi \sin\theta/\lambda$, λ is the incident wavelength, θ is the half of the scattering angle, ϕ is the volume fraction of the particles in the solution, ρ_1 is the electron density of the particle, ρ_2 is the electron density of the surrounding medium, and $P(q)$ is the particle form factor. For randomly oriented platelets of width T, the factor $P(q)$ can be written as

$$P(q) = \frac{I_0}{q^2}\exp\left(-\frac{T^2q^2}{12}\right) \quad (2)$$

It follows

$$I(q)q^2 \propto \exp\left(-\frac{T^2q^2}{12}\right) \quad (3)$$

According to eq 3, a plot of experimental log[$I(q)q^2$] vs q^2 data is a straight line, with a slope m related to the thickness value by[43]

$$T = \sqrt{-12m\ln(10)} \quad (4)$$

The Guinier plots presenting the change of log[$I(q)q^2$] vs q^2 plots for raw and intercalated Laponites are shown in Figure 3. The values of T were calculated in the q range indicated. In this region, we can assume that $S(q) = 1$ and that the scattering intensity is determined solely by the form factor, $P(q)$, which is function of the particle dimensions (size and shape). The results are shown in Table 2.

The thickness obtained for raw Laponite by this analysis is in good agreement with the data published by Ramsay,[44] who found for this system particles with an approximate thickness of 10 Å. In the case of the organically modified Laponite samples, the slope increases with increasing AIBA loading, thus indicating an increase in the thickness of the scatterering platelets. As mentioned above, once AIBA molecules are introduced in the Laponite suspensions, these organic cations can interact with the surface of Laponite and form interlayer complexes.[45] The values for T correspond to an average of two or three clay platelets (each of 1 nm of thickness) separated by AIBA molecules of 4 nm thickness. The higher particle thickness is exhibited by the AIBA-Lap-200 system. These

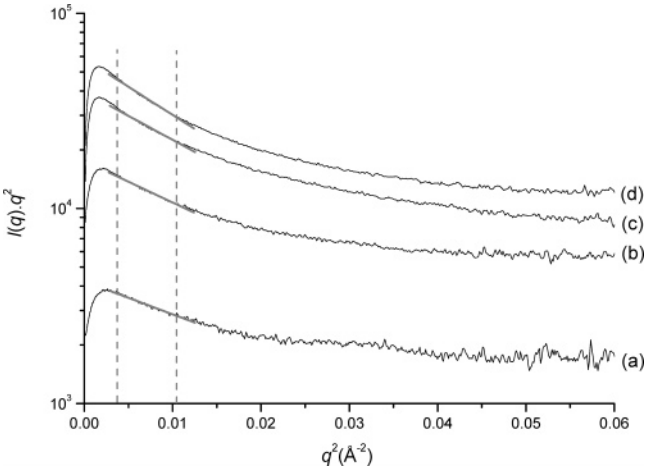

Figure 3. Plot of log $I(q)q^2$ vs q^2 for raw and modified Laponite: (a) Laponite RD, (b) AIBA-Lap-57, (c) AIBA-Lap-118, and (d) AIBA-Lap-200. The dotted line shows the q range used for the determination of the platelet thickness with Guinier's law (solid gray lines).

Table 2. Guinier Thickness of Raw Laponite Solutions and of AIBA−Laponite Intercalation Complexes Solutions Containing Increasing Amounts of AIBA

sample	C_{AIBA} adsorbed (mmol g$^{-1}_{Laponite}$)	slope (m)	T (Å)
Laponite RD	0	−16	12
AIBA-Lap-57	0.21	−22	17
AIBA-Lap-118	0.35	−26	24
AIBA-Lap-200	0.37	−30	32

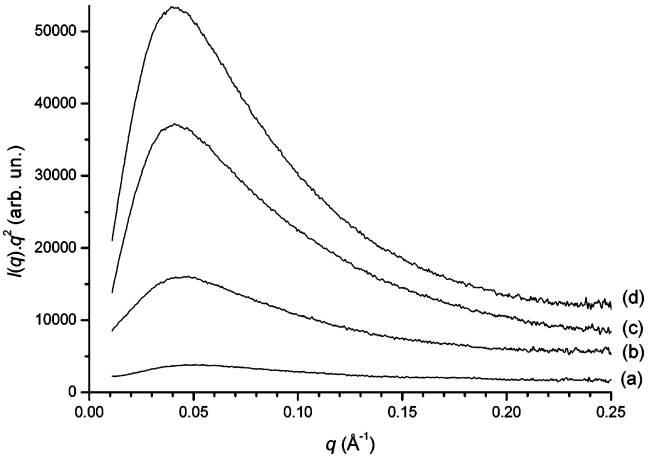

Figure 4. Plot of $I(q)q^2$ vs q in the low q range for raw and organically modified Laponite: (a) Laponite RD, (b) AIBA-Lap-57, (c) AIBA-Lap-118, and (d) AIBA-Lap-200. All samples, including Laponite RD with no tactoids, display a correlation peak.

results clearly illustrate the effect of the cation exchange on the structure of the clay platelets in aqueous suspensions and are in qualitative agreement with the dynamic light scattering measurements shown above.

At lower q values, the log[$I(q)q^2$] vs q^2 plots exhibit a maximum, corresponding to an interparticulate distance or correlation distance, d^*. This interpretation was previously given by several authors,[46−48] and we calculated d^* on the basis of the phenomenological use of the Bragg equation. The scattering vector in SAXS is given by $q = (4\pi/\lambda)\sin(\theta)$ and $\lambda = 2d\sin(\theta)$, leading to $d^* = 2\pi/q_{max}$. As shown in Figure 4, the raw Laponite exhibits a peak in the Kratky plot (log[$I(q)q^2$] vs q) at $q \approx 0.051$ Å^{-1}. After cation exchange, this peak shifts to lower q values, indicating an increase in the interparticulate distance. This should be related to a decrease of the number of platelets as a consequence of intercalated AIBA.

Table 3. Location of the Maximum of the Scattering Factor $S(q)$ and Corresponding Interparticle Distances as a Function of the Laponite Treatment

sample	C_{AIBA} adsorbed (mmol $g^{-1}_{Laponite}$)	q (Å^{-1})	d (Å)
Laponite RD	0	0.052	121
AIBA-Lap-57	0.21	0.045	140
AIBA-Lap-118	0.35	0.042	150
AIBA-Lap-200	0.37	0.041	155

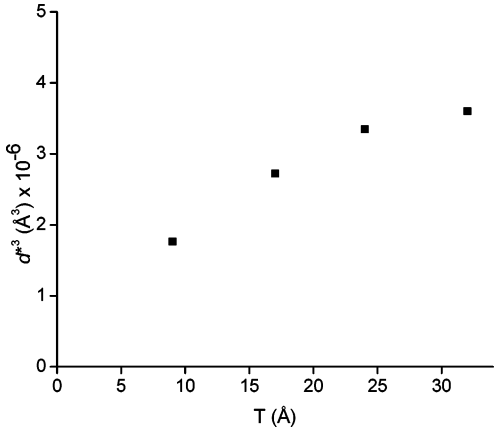

Figure 5. Evolution of the characteristic distance between platelets in the solution d^* (calculated from the position of the correlation peak) vs the width of the platelets T in the case of Laponite suspensions (data from Tables 1 and 2).

The values of d^* are shown in Table 3. Again, this result suggests that the scattering objects are made of stacks of individual platelets when the Laponite is modified since a complete exfoliated situation would lead to a higher number of platelets with smaller interparticle distances. Similar results have been observed in the case of Montmorillonite intercalated with hexadecyltrimethylammonium ions.[49]

To go one step further, we followed the evolution of T and d^* in the same plot in order to describe the state of dispersion of Laponite RD in water. Figure 5 displays the evolution of d^{*3} with T. In perfectly diluted conditions, the volume fraction φ_v should be related to the average volume of a platelet v_m and the interdistance platelet d^* by

$$\varphi_v \approx v_m/(d^*)^3 = \pi R^2 T/(d^*)^3 \qquad (5)$$

Thus, the plot of $(d^*)^3$ vs T should exhibit a straight line. This is the case only in the high exfoliation limit and should be verified at much lower clay concentrations.

Indeed, the slope of the $d^{*3}-T$ plot can be related to the characteristic surface $\pi R^2/\varphi_v \sim 2\pi R^2/\varphi_m$. The corresponding value of R is much lower than the expected radius of the Laponite disks, thus indicating that an orientation correlation of neighboring platelets is present at this Laponite concentration (10 g/L). Such orientation correlation is indeed one of the key features of several models for clay suspensions.[47] This can also be deduced from the absolute value of d^* (see Table 2), which is comparable to, but lower than, the lateral size of Laponite disks (300 Å). More structural investigations at lower concentrations are thus needed to verify the parameters to be introduced in eq 5.

Nanocomposite Latexes. AIBA-functionalized Laponite particles prepared under the optimal conditions described earlier were used as seeds to synthesize a series of nanocomposite latexes. As described in a previous work,[11] sonication resulted in the formation of a milky suspension that remained stable for several hours. However, attempts to determine the droplet diameter by DLS were unsuccessful suggesting only a limited stability of the resulting "mini"emulsion. The emulsion was introduced into the reactor and bubbled with nitrogen for 10 min before increasing the temperature to 70 °C to start polymerization. In all cases, a milky white dispersion with no evidence of any macroscopic precipitation was obtained, in contrast to preliminary experiments performed using a conventional emulsion polymerization recipe. Full conversions were achieved in a short period of time (around 30 min) and with a good reproducibility. The resulting latexes will be referred hereafter to as NL-AIBA-57, NL-AIBA-118, and NL-AIBA-200, respectively.

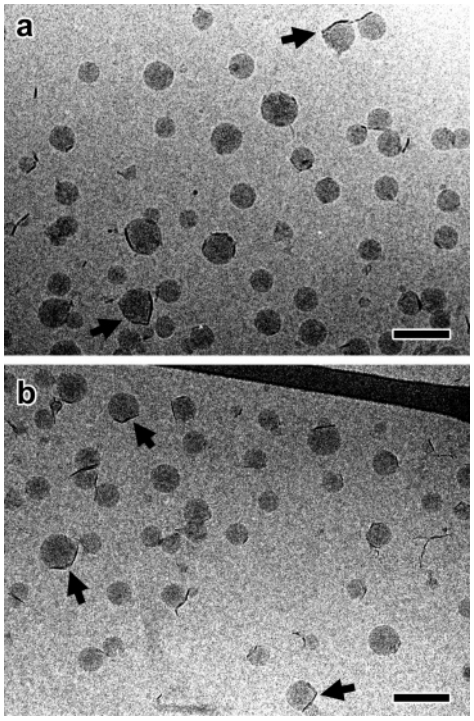

Figure 6. Cryo-TEM images of NL-AIBA-57 nanocomposite particles (scale bars: 100 nm). The arrows indicate a faceting effect induced by the rigidity of Laponite platelets seen edge-on with respect to the observation direction.

Figure 6 shows cryo-TEM images of individual NL-AIBA-57 spherical nanoparticles, with a diameter ranging from 30 to 70 nm and a relatively narrow size distribution. Dark "filaments" are observed on the surface of some particles. As explained in a previous paper,[10a] they correspond to Laponite crystallites seen edge-on with respect to the observation direction and exhibiting a strong diffraction contrast. Laponite platelets with a different orientation do not generate much contrast and can hardly be detected in the images. On the largest particles, a faceting effect is clearly observed, likely induced by the rigidity of the clay platelets. The fact that this faceting is only observed on some parts of the particles strongly suggests that the covering of the surface is only partial. Nevertheless, it appears that only a few modified Laponite crystallites contain enough AIBA molecules to initiate the polymerization of monomers and generate a polymer latex particle.

Cryo-TEM micrographs of NL-AIBA-118 nanocomposite particles are shown in Figure 7. Three different populations of particles corresponding to different diameters are observed. The smallest (~40 nm) polymer particles seem to have very few Laponite platelets on their surface. A larger number of clay platelets are seen on 60−80 nm nanospheres, but the covering is still partial. Finally, bigger and darker particles (>100 nm) appear to be continuously covered by Laponite. Their shape is

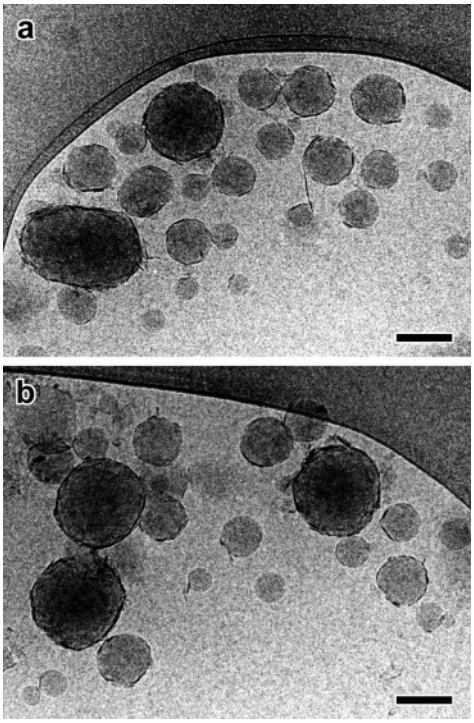

Figure 7. Cryo-TEM images of NL-AIBA-118 nanocomposite particles (scale bars: 100 nm).

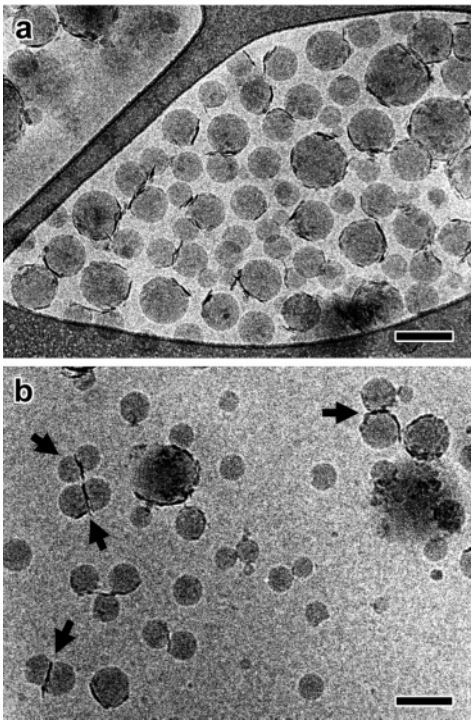

Figure 8. Cryo-TEM micrographs of NL-AIBA-200 nanocomposite particles (scale bars: 100 nm). The arrows indicate objects corresponding to the association of two polymer particles that have developed on both faces of Laponite platelets.

not always perfectly spherical (Figure 7a), either because of some deformation undergone in the liquid film during preparation or because of some rigidity locally induced by the Laponite surface. In some cases, small (30−50 nm) polymer nanospheres seem to have developed on the outer clay surface of the larger particles.

Figure 8 shows the morphology of the NL-AIBA-200 particles. By comparison with the NL-AIBA-118 sample, the covering of polymer particles is only partial and rather heterogeneous. A new population of objects is observed showing polymer particles developing on both faces of the Laponite platelets (Figure 8b). Finally, it is worth mentioning an increase in both the population of small particles without modification and in the concentration of impurities.

Scheme 1. Scheme Illustrating the Possible Relationship between the Cation Exchange Process and Particles Morphology: (a) AIBA Concentrations below the CEC and (b) above the CEC

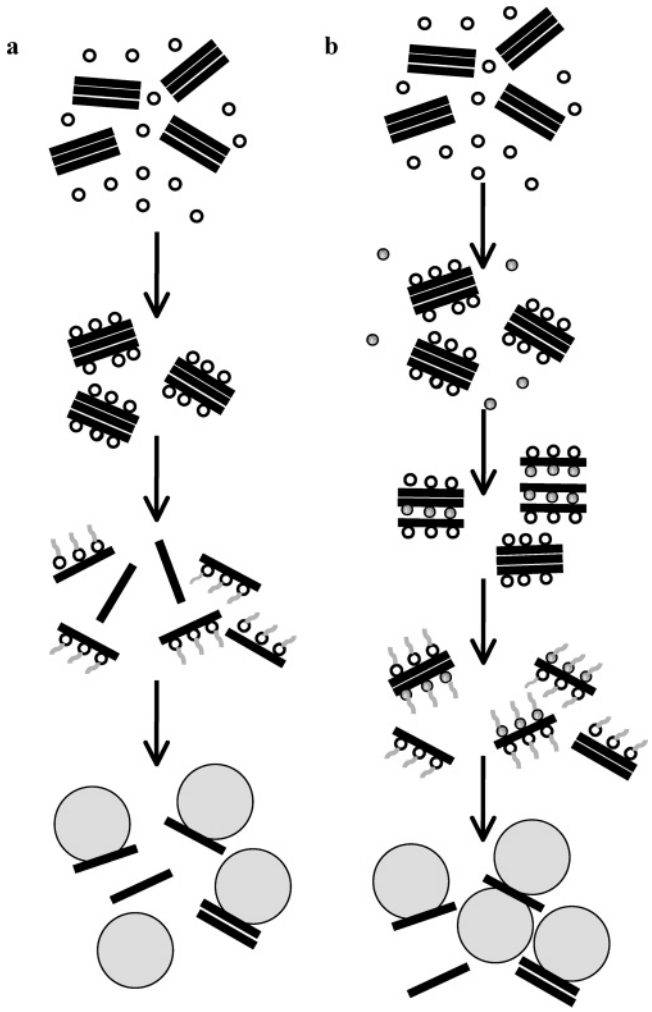

Effect of AIBA Loading. As clearly seen from the cryo-TEM images, the distribution of Laponite at the surface of the latex particles and the resulting morphology strongly depend on the amount of AIBA that is initially introduced in the clay suspension. A close inspection of the hybrid particles obtained in the different situations allowed us to propose the following scenarios to account for the different morphologies.

First, it should be pointed out that when AIBA is introduced in the clay suspension, a sudden increase in the ionic strength and the rapid neutralization of the surface charges of Laponite promote the formation of small tactoids made of three or four clay sheets stacked together as supported by SAXS analysis. Therefore, it can be assumed that in the very first seconds after the addition of AIBA, agregation takes place in such a way that the AIBA molecules can no longer have access to the clay interlayer region. AIBA thus selectively adsorbs on the external surface of the tactoids, as schematically illustrated in Scheme 1. However, after redispersion into water by sonication, deagglomeration of the clay tactoids may liberate new surfaces in such a way that readsorption can take place on these freshly

exposed surfaces, including the interlamellar region of the clay particles as represented in Scheme 1a. However, this supposes that AIBA adsorption does not take place on two adjacent clay layers as this would result in pinning of the clay stacks which process would be irreversible. Nevertheless, the possibility that some clay layers are chemically linked together by the AIBA molecules cannot be completely excluded at the present time, and this hypothesis may account for the remaining presence of some large clay aggregates after redispersion into water. At loadings below the CEC of the clay (AIBA-Lap-57), all of the AIBA cations have already been associated with the clay surface, and no free molecules are available to readsorb into the interlayer region (Scheme 1a). Consequently, the clay platelets are selectively functionalized on only one side. The polymer latex particles are thus expected to grow from the side of the clay platelets onto which the AIBA molecules had been selectively adsorbed. This assumption is supported by the cryo-TEM observations (Figure 6). In the case of AIBA-Lap-118 and AIBA-Lap-200, the presence of free AIBA enables readsorption to take place into the interlamellar region of the clay particles after sonication and redispersion into water. Therefore, in these particular situations, we observed a new population of dumbbell-like composite latex particles characterized by clay platelets sandwiched between two polymer spheres that have grown from the opposite sides of Laponite (Scheme 1b). According to this scenario, the higher the AIBA concentration, the more important is the probability to observe this last type of sandwich morphology, in agreement with cryo-TEM observations (Figures 7 and 8).

In addition to differences in particle morphology, cryo-TEM images also show differences in particle size and size distribution that cannot be explained by the above scenario. While the particles synthesized using AIBA-Lap-57 are rather monodisperse, those produced from the AIBA-Lap-118 or AIBA-Lap-200 intercalation complexes are much more polydisperse and exhibit a broader variety of morphologies. In our opinion, the morphology of the composite particles strongly depends on the quality of the aqueous clay dispersion involved in the polymerization reaction. Indeed, it should be recalled that for low AIBA loadings the organoclay could be satisfactorily dispersed into water and displayed an average diameter of ca. 50 nm, which value is close to the diameter of fully exfoliated Laponite. In contrast, when the amount of AIBA was increased, the particle size and size distribution of the organoclay got broader with average diameters of ca. 105 and 180 nm for Lap-AIBA-118 and Lap-AIBA-200, respectively. As evidenced by SAXS analysis, these suspensions are made up of stacky aggregates of clay layers. It is noteworthy that the larger the Laponite particle size, the larger the size and size distribution of the composite particles. On the basis of these observations, it can be assumed that there is a relationship between the state of clay dispersion and particle morphology. Let us describe in more detail what is taking place in the present system. Polymerization starts in the aqueous phase through the decomposition of the initiator moieties attached to the clay surface. The growth of the oligomeric radical then proceeds at the surface of Laponite by the addition of monomers dissolved in water and propagation of radicals. In the case of the NL-AIBA-57 nanocomposites, the Laponite particles are well dispersed, and separation of the Laponite layers allows the particles to grow from the individual clay sheets, thus resulting in a small increment of particles size. However, in the case of NL-AIBA-118 and NL-AIBA-200 where there are big aggregates present in the suspension at the beginning of polymerization, the growth of polymer particles at the surface of these aggregates results in the formation of larger particles, as illustrated in Scheme 2. The particle size distribution and the variety of morphology thus seem to be related to the diversity of aggregation states which are present in the clay suspension.

Scheme 2. Scheme of the Possible Formation of Nanocomposites at Different Levels of Modification of Laponite with AIBA

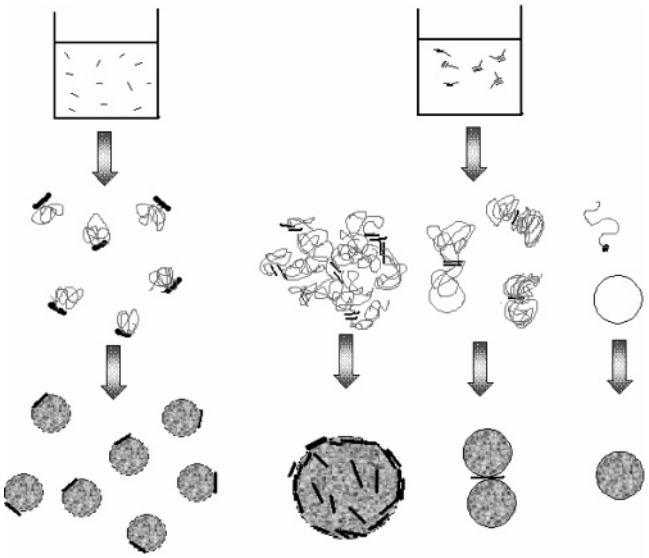

Conclusions

A series of poly(Sty-*co*-BuA)/Laponite composite latexes have been synthesized through emulsion polymerization. The clay layers were first functionalized by cation exchange of the sodium ions with a diazoic initiator (AIBA). The ion-exchanged Laponites containing increasing amounts of AIBA were redispersed into water with the help of ultrasound in the presence of $Na_4P_2O_7$ and SDS. DLS measurements showed that the lowest particle size was achieved by stirring the suspension for a period of time ranging from 1 to 5 days depending on the AIBA concentration. SAXS analysis revealed that the suspensions were made of stacky agglomerates containing from three to four individual platelets. The emulsion polymerization was performed in the presence of the organoclay which played the role of a solid initiator. This resulted in the formation of composite latexes which surface was recovered by the clay platelets. Cryo-TEM showed that the level of organic modification of Laponite played an important role in the morphology of the composite particles. The higher the amount of intercalated AIBA, the larger the size and size distribution of the clay aggregates and the greater the diversity of particle morphology.

Acknowledgment. The authors are grateful to the CONACYT for its financial support to this work. The gift of a sample of Laponite RD by Rockwood Additives is also greatly acknowledged.

References and Notes

(1) Pomogalio, A. D. *Russ. Chem. Rev.* **2000**, *69*, 53−80.
(2) Kickelbick, G. *Prog. Polym. Sci.* **2003**, *28*, 83−114.
(3) Castelvetro, V.; De Vita, V. C. *Adv. Colloid Interface Sci.* **2004**, *108*−*109*, 167−185.
(4) Bourgeat-Lami, E. *J. Nanosci. Nanotechnol.* **2002**, *2*, 1−24.
(5) Bourgeat-Lami, E. In *Encyclopedia of Nanoscience and Nanotechnology*; American Scientific Publishers: Los Angeles, 2004; Vol. 8, pp 305−332.
(6) Lagaly, G. *Appl. Clay Sci.* **1999**, *15*, 1−9.
(7) Alexandre, M.; Dubois, P. *Mater. Sci. Eng.* **2001**, *28*, 1−63.

(8) Ray, S. S.; Okamoto, M. *Prog. Polym. Sci.* **2003**, *28*, 1539−1641.
(9) Utracki, L. A. *Clay-Containing Polymeric Nanocomposites*; Rapra Technology Limited: Shropshire, UK, 2004.
(10) (a) Negrete-Herrera, N.; Letoffe, J.-M.; Putaux, J.-L.; David, L.; Bourgeat-Lami, E. *Langmuir* **2004**, *20*, 1564−1571. (b) Negrete-Herrera, N.; Letoffe, J.-M.; Reymond, J.-P.; Bourgeat-Lami, E. *J. Mater. Chem.* **2005**, *15*, 863−871.
(11) Negrete-Herrera, N.; Persoz, S.; Putaux, J.-L.; David, L.; Bourgeat-Lami, E. *J. Nanosci. Nanotechnol.* **2006**, *6*, 421−431.
(12) Moet, A. S.; Akelah, A. *Mater. Lett.* **1993**, *18*, 97−102.
(13) Akelah, A.; Moet, A. S. *J. Mater. Sci.* **1996**, *31*, 3589−3596.
(14) Fu, X.; Qutubuddin, S. *Mater. Lett.* **2000**, *42*, 12−15.
(15) Fu, X.; Qutubuddin, S. *Polymer* **2001**, *42*, 807−813.
(16) Dietsche, F.; Thomann, Y.; Thomann, R.; Mülhaupt, R. *J. Appl. Polym. Sci.* **2000**, *75*, 396−405.
(17) Tabtiang, A.; Lumlong, S.; Venables, R. A. *Eur. Polym. J.* **2000**, *36*, 2559−2568.
(18) Shengpei, S.; Jiang, D. D.; Wilkie, C. A. *Polym. Adv. Technol.* **2004**, *15*, 225−231.
(19) Choi, Y. S.; Choi, M. H.; Wang, K. H.; Kim, S. O.; Kim, Y. K. *Macromol.* **2001**, *34*, 8978−8985.
(20) Al-Esaimi, M. M. *J. Appl. Polym. Sci.* **1997**, *64*, 367−372.
(21) Lee, D. C.; Jang, L. W. *J. Appl. Polym. Sci.* **1996**, *61*, 1117−1122.
(22) Lee, D. C.; Jang, L. W. *J. Appl. Polym. Sci.* **1998**, *68*, 1997−2005.
(23) Noh, M. W.; Jang, L. W.; Lee, D. C. *J. Appl. Polym. Sci.* **1999**, *74*, 179−188.
(24) Noh, M. W.; Lee, D. C. *J. Appl. Polym. Sci.* **1999**, *74*, 2811−2819.
(25) Noh, M. W.; Lee, D. C. *Polym. Bull. (Berlin)* **1999**, *42*, 619−626.
(26) Bandyopadhyay, S.; Giannelis, E. P.; Hsieh, A. J. *PMSE Prepr.* **2000**, *82*, 208−209.
(27) Huang, X.; Brittain, W. J. *Polym. Prepr.* **2000**, *41*, 521−522.
(28) Huang, X.; Brittain, W. J. *Macromolecules* **2001**, *34*, 3255−3260.
(29) Chen, G.; Ma, Y.; Qi, Z. *Scr. Mater.* **2001**, *44*, 125−128.
(30) zu Putlitz, B.; Landfester, K.; Fischer, H.; Antonietti, M. *Adv. Mater.* **2001**, *13*, 500−503.
(31) Meneghetti, P.; Qutubuddin, S. *Langmuir* **2004**, *20*, 3424−3430.
(32) Bourgeat-Lami, E.; Negrete-Herrera, N.; Putaux, J.-L.; Reculusa, S.; Perro, A.; Ravaine, S.; Mingotaud, C.; Duguet, E. *Macromol. Symp.* **2005**, *229*, 32−46.
(33) Dubochet, J.; Adrian, M.; Chang, J.-J.; Homo, J. C.; Lepault, J.; McDowall, A. W.; Schultz, P. Q. *Rev. Biophys.* **1988**, *21*, 129−228.
(34) Harris, J. R. *Negative Staining and Cryoelectron Microscopy: The Thin Films Techniques*; Bios Scientific Publishers: Oxford, UK, 1997.
(35) Durrieu, V.; Gandini, A.; Belcacem, M. N.; Blayo, A.; Eiselé, G.; Putaux, J.-L. *J. Appl. Polym. Sci.* **2004**, *94*, 700−710.
(36) Mourchid, A.; Lécolier, E.; van Damme, H.; Levitz, P. *Langmuir* **1998**, *14*, 4718−4723.
(37) Cases, J.-M. *Chim. Phys.* **1969**, *66*, 1602.
(38) Thompson, D. W.; Butterworth, J. T. *J. Colloid Interface Sci.* **1992**, *151*, 236−243.
(39) Bourlinos, A.; Jiang, D.; Giannelis, P. *Chem. Mater.* **2004**, *16*, 2404−2410.
(40) Porion, P.; Al-Mukhtar, M.; Faugère, A. M.; Delville, A. *J. Phys. Chem. B* **2004**, *108*, 10825−10831.
(41) Guinier, A.; Fournet, G. *Small Angle Scattering of X-rays*; Wiley: New York, 1955.
(42) Morvan, M.; Espinat, D.; Lambard, R.; Zemb, T. *Colloids Surf., A* **1994**, *82*, 193−203.
(43) Cebula, D. J.; Thomas, R. *Faraday Discuss. Chem. Soc.* **1978**, *65*, 76.
(44) Ramsay, D. F. *J. Colloid Interface Sci.* **1986**, *109*, 441−447.
(45) McBride, M. B. *Surface Chemistry of Soils Minerals*, 2nd ed.; SSSA Book Ser. 1; Soil Science Society of America: Madison, WI, 1989.
(46) Ramsay, J. D. F.; Swanton, S. W.; Bunce, J. *J. Chem. Soc., Faraday Trans.* **1990**, *86*, 3919.
(47) Morvan, M.; Espinat, D.; Lambard, J.; Zemb, Th. *Colloids Surf., A* **1994**, *82*, 193.
(48) Saunders, J. M.; Goodwin, J. W.; Richardson, R. M.; Vincent, B. *J. Phys. Chem. B* **1999**, *103*, 9211.
(49) Shang, C.; Rice, J. A.; Lin, J. S. *Soils Sci. Soc. Am. J.* **2002**, *66*, 1225−1230.

MA0610515